

Masked Training for Robust Arrhythmia Detection from Digitalized Multiple Layout ECG Images

Shanwei Zhang^{1,6,✉}, Deyun Zhang^{2,✉}, Yirao Tao³, Kexin Wang¹, Shijia Geng², Jun Li^{6,7}, Qinghao Zhao⁴, Xingpeng Liu³, Yuxi Zhou^{1,5,*}, and Shenda Hong^{6,7,*}

¹Department of Computer Science, Tianjin University of Technology, Tianjin, China

²HeartVoice Medical Technology, Hefei, China

³Department of Cardiology, Beijing Chaoyang Hospital, Capital Medical University, Beijing, China

⁴Department of Cardiology, Peking University People's Hospital, Beijing, China

⁵DCST, BNRist, RIIT, Institute of Internet Industry, Tsinghua University, Beijing, China

⁶National Institute of Health Data Science, Peking University, Beijing, China

⁷Institute for Artificial Intelligence, Peking University, Beijing, China

*Correspondence: joy_yuxi@pku.edu.cn, hongshenda@pku.edu.cn

ABSTRACT

Electrocardiogram (ECG) as an important tool for diagnosing cardiovascular diseases such as arrhythmia. Due to the differences in ECG layouts used by different hospitals, the digitized signals exhibit asynchronous lead time and partial blackout loss, which poses a serious challenge to existing models. To address this challenge, the study introduced PatchECG, a framework for adaptive variable block count missing representation learning based on a masking training strategy, which automatically focuses on key patches with collaborative dependencies between leads, thereby achieving key recognition of arrhythmia in ECGs with different layouts. Experiments were conducted on the PTB-XL dataset and 21388 asynchronous ECG images generated using ECG image kit tool, using the 23 Subclasses as labels. The proposed method demonstrated strong robustness under different layouts, with average Area Under the Receiver Operating Characteristic Curve (AUROC) of 0.835 and remained stable (unchanged with layout changes). In external validation based on 400 real ECG images data from Chaoyang Hospital, the AUROC for atrial fibrillation diagnosis reached 0.778; On 12 x 1 layout ECGs, AUROC reaches 0.893. This result is superior to various classic interpolation and baseline methods, and compared to the current optimal large-scale pre-training model ECGFounder, it has improved by 0.111 and 0.19.

KEYWORDS

Deep Learning, Masked Training, Multiple Layout ECG Images, Digitalized ECG

INTRODUCTION

Cardiovascular disease (CVD) is one of the world's deadliest disease, causing approximately 17.8 million deaths according to 2017 statistics¹. Electrocardiogram (ECG) is a key tool for the diagnosis and treatment of CVD, revealing important pathophysiological information by recording the electrical activity of the heart. In recent years, deep learning techniques have been shown to rival trained doctors in ECG signal and ECG arrhythmia detection tasks. Despite recent advances in digital ECG equipment, the use of photographs, printed screens, or paper ECGs is still prevalent in the Global South, where ECG slices are far less expensive to store than signal data, and where these recordings not only contain a rich history of CVD, but also reflect its diversity. In underdeveloped regions, this non-digitized data format highlights the urgent need for

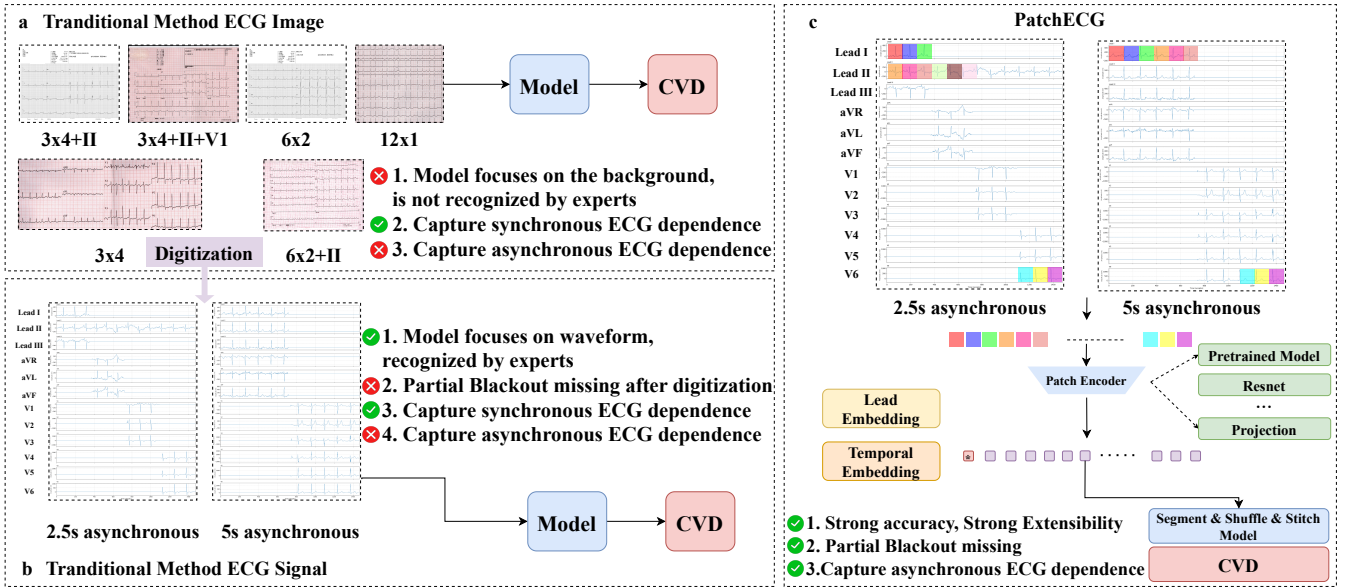


Figure 1: **a**: Traditional image methods focus on the image background and are limited in accuracy, and cannot effectively capture asynchronous ECG dependencies. **b**: Signal methods are highly accurate, cannot capture asynchronous asynchronous ECG dependencies and effectively deal with partial blackout missing. **c**: We propose a variable block number mechanism and patch guided attention mechanism based on masking training adaptation, which can effectively handle ECG with different layouts.

high-quality digitization and automated analysis tools². Thus, digitizing traditional ECG images and building algorithms capable of automated diagnosis based on them will both help to deepen our understanding of CVD and, hopefully, significantly improve the diagnosis and treatment of underrepresented and medically under-resourced populations.

ECG images exist in a variety of layouts. For example, in Fig. 1(a), different forms such as common 3 × 4 + II layout, 6 × 2 layout or complete 12-lead may be presented. In existing studies, ECG images with different layouts are usually directly inputted into an image classification model for classification^{3,4}. Data augmentation (e.g., rotation, folding, light and shadow adjustments, disrupting lead positions, etc.) of such images can effectively improve the robustness of the model so that it still maintains a high accuracy in predicting real-world data. Data augmentation (e.g., rotation, folding, light and shadow adjustments, disrupting lead positions, etc.) of such images can effectively improve the robustness of the model so that it still maintains a high accuracy in predicting real-world data. However, image classification models are prone to focus excessively on the image background rather than the ECG signal itself. Although ECG all-in-one⁴ provides more accurate interpretability by calculating the classifier gradient through Jacobi matrix sensitivity, its interpretation results still focus on the image background. This tends to raise questions from experts about its interpretability, as physicians have more confidence in the prediction results based on the ECG signal itself than the image model.

With the development of methods for digitizing ECG images, ECG image data can be accurately converted into ECG signal data^{5,6}, making it possible to use the signal data for subsequent analysis. As shown in Fig. 1(b), the digitization of ECG image with different layouts of image produces 2.5s asynchronous, 5s asynchronous and synchronous signals⁷ and “Partial Blackout” which covers situations where a variable number of features become unavailable for some time⁸. This digitized signal ECG presents two major challenges:

- There are differences in the way ECG images are stored in different hospitals, such as the common 3 × 4 or 6 × 2 layouts. After digitizing these images, the signal data are often missing

to varying degrees of partial blackout. It remains a challenging task to effectively model multi-lead ECG data with partial blackout without relying on additional interpolation (avoid introducing noise) and preserving the original information as much as possible.

- Existing methods usually assume that multilead ECG signals are synchronized; however, after digitization of different layouts of ECG images, the signals of each lead appear to be inconsistently missing in time, resulting in asynchronous ECGs of 2.5s or 5s. Current methods, whether based on image or signal level, are difficult to capture the synergistic dependencies and temporal features among multiple leads in this asynchronous mode, and achieving effective modeling is still a challenge to be solved.

To overcome these challenges, We propose PatchECG—a framework based on a masked training strategy and not relying on additional interpolations that can be adapted to different layouts of ECGs. The main contributions of this study are as follows:

- Aiming at the missing problem due to different layouts, we design an adaptive variable block number missing learning mechanism. Combined with a masked training strategy, it is able to directly model the missing regions without relying on any interpolation operation, effectively capturing the temporal features and synergistic dependencies among multiple leads.
- In order to capture the complex structure of ECG with different layouts, we construct a disordered patch attention mechanism to encode patches and introduce patch-level temporal-lead embedding. We automatically focus on the important segments that have synergistic dependencies between leads in terms of timing, thus realizing the intelligent recognition of arrhythmia in any ECG layout.
- We test on ECG images collected at Chaoyang Hospital. The images were converted into signal data by digitization methods and based on which external validation was performed. The results show that our method is effective in capturing critical patches and making accurate diagnosis. In particular, on the external validation cohort of AF ECG images from Chaoyang Hospital, the model evaluation achieved an AUROC of 0.778, which effectively demonstrates the ability of the method to identify the key patches and achieve an accurate diagnosis of AF.

RESULTS

To comprehensively evaluate the performance of our proposed PatchECG, we conducted a series of rigorous experiments and we conducted a series of rigorous experiments and compared it with several key baseline models, including: 1) The typical baseline⁹ in the main follow MissTSM paper uses zero padding, KNN interpolation, and SAITS interpolation¹⁰, respectively, and combines them with SimMTM for prediction¹¹; 2) Medformer is a model specifically designed for biosignals, which introduces six different noise perturbations intra- and inter-granularity during the training phase, thus enhancing robustness to missing¹²; 3) TimeXer, on the other hand, provides auxiliary cues to the model by explicitly modeling missing patterns and treating the missing as a kind of external information¹³. We explored the diagnostic accuracy of the generated signal data digitized from ECG images by different layouts of signal data and the signal data digitized from different layouts of ECG images from the real Chaoyang Hospital.

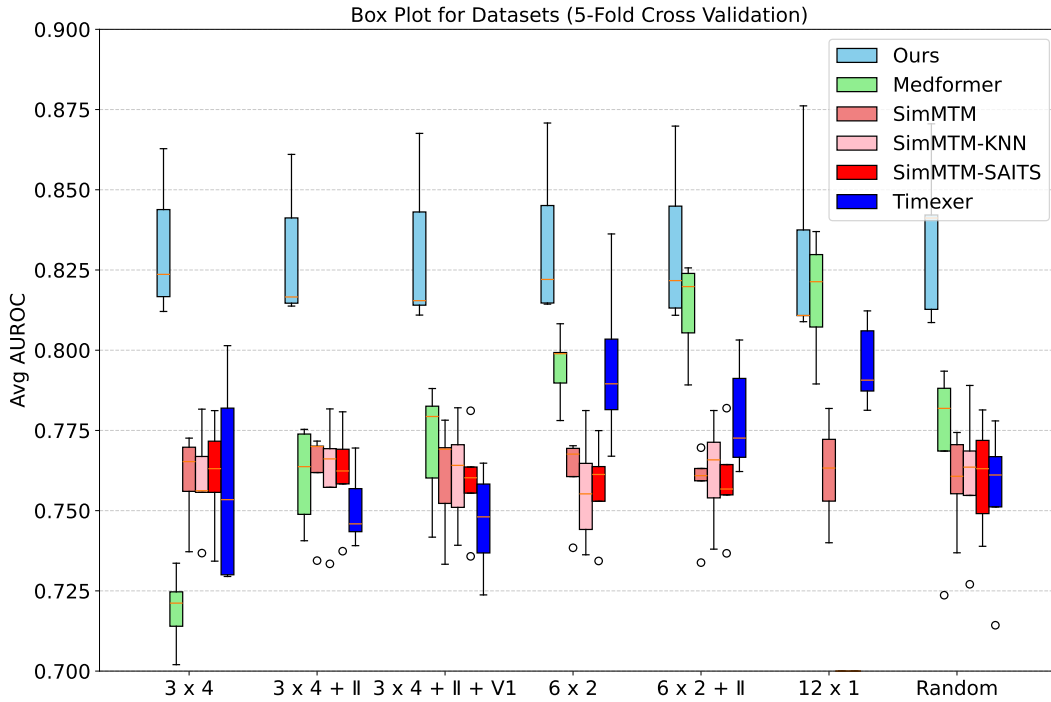


Figure 2: Results of PatchECG and Other Methods with Different Layouts

PatchECG Achieve Better Results on Different Layouts

As shown in Figure 2, our method obtained optimal average AUROC performance with 5-fold cross-validation under different ECG layouts. In the comparison with multiple baseline methods, we did not use the interpolation strategy due to the fact that interpolation may introduce hard-to-interpret noise and reduce the interpretability of the model. The experimental results show that the interpolation methods of zero padding, KNN and SAITS may introduce different degrees of noise interference under different layouts, and the model performance is similar, with the average AUROC mostly centered in the 0.750-0.775 range, and the different interpolation methods can not bring effective performance improvement. With the variation in lead layouts, Medformer performs better under more complete lead layouts, with its average AUROC showing an upward trend, and it performs comparably to our method in the 12×1 complete lead layouts. The performance of TimeXer is inferior in 3×4 layout compared to 6×2 layout. This is due to the missing of longer time segments in the 3×4 layout, leading to a higher number of consecutive token losses. Consequently, this affects the model’s ability to capture temporal features, resulting in a relative decline in performance.

PatchECG is Highly Scalable

To effectively utilize existing excellent models, we explored three different modules for encoding patches. We primarily adopted representative models such as Net1D, ECGFounder, and Projection as PatchEncoders: 1. Net1D: a residual one-dimensional convolutional model combined with an SE module¹⁴. 2. ECGFounder: the latest foundational model pre-trained on 10 million ECGs; we froze its parameters and used it as a PatchEncoder to encode patches¹⁵. 3. Projection: inspired by PatchTST, it performs simple projection on patches through a fully connected layer¹⁶.

We adopted the same training, validation, and test set partitions as in Experiment 1 and conducted 5-fold cross-validation. As shown in Table 1, due to the advantages of the method, we can use different modules as PatchEncoders. When dealing with multi-label classification tasks

Table 1: Different modules as PatchEncoder

Method	3 x 4	3 x 4 + II	3 x 4 + II + V1	6 x 2	6 x 2 + II	12 x 1	Random
Ours-Projection	0.768 ± 0.034	0.781 ± 0.037	0.782 ± 0.034	0.790 ± 0.032	0.792 ± 0.032	0.784 ± 0.028	0.780 ± 0.037
Ours-Resnet	0.831 ± 0.019	0.829 ± 0.019	0.830 ± 0.022	0.833 ± 0.022	0.832 ± 0.022	0.829 ± 0.026	0.835 ± 0.022
Ours-ECGFounder	0.876 ± 0.027	0.872 ± 0.026	0.875 ± 0.028	0.879 ± 0.025	0.881 ± 0.026	0.882 ± 0.024	0.872 ± 0.027

under different layouts, the model effectively captures the asynchronous signal dependencies caused by layouts differences. Therefore, even if the input signal layouts vary, the model can still achieve a close average AUROC across different layouts. A detailed analysis of the performance of each PatchEncoder module is as follows: Projection: Due to its simple structure, it is difficult to learn complex information about patches, making it the worst performing as a PatchEncoder. Net1D: Trained from scratch, it achieved a more robust average AUROC performance in testing after 5-fold cross-validation, achieving the second-best result. Large-scale ECG pre-trained model (ECGFounder): Its parameters were frozen and directly used for patch encoding, achieving the best average AUROC. In summary, our method can effectively utilize existing excellent models (including large-scale pre-trained models) as PatchEncoder, combined with an adaptive variable block number missing mechanism, enabling PatchECG to maintain high accuracy when processing both asynchronous and synchronous ECG data.

PatchECG Achieve Better Results on Generating ECG Images

To further verify the adaptability of the model in complex real-world scenarios, the ECG-image-kit tool was used to generate ECG images. During the image generation process, common practical interference factors were simulated, and noises such as rotation, wrinkling, and light and shadow changes were added to more realistically reproduce images in clinical settings. Due to limitations of the tool itself, the generated ECGs adopted a 3 × 4 layout. Subsequently, the generated ECG images were subjected to signal reconstruction using the digital method that won first place in the George B. Moody PhysioNet Challenges 2024⁵. The digitized signals were used as inputs for model testing, and the labels used in the testing phase were consistent with those used in the training phase. We adopted the AUROC as the evaluation metric and used 5-fold cross-validation to improve the stability and reliability of the results. The experimental results are shown in Figure 3.

When the digitized signal obtained from the generated ECG image is used as the model input, our method performs the best among all baseline methods. Due to the high accuracy of digitization, TimeXer can effectively capture the exogenous information provided by the missing patterns, thus demonstrating excellent performance in this experiment. In contrast, MedFormer performs poorly under this layout, mainly because the 3 x 4 layout is the one that loses the most information, making it difficult for the model to obtain complete features, thus becoming the worst-performing baseline method in this experiment. Furthermore, other imputation-based baseline methods, whether using KNN imputation, SAITS imputation, or zero padding, perform almost equally well due to the introduction of additional noise in the missing areas. Different imputation methods do not bring significant improvements to the model.

PatchECG Achieve Better Results on Real Hospital ECG Images

On the external test set of Chaoyang Hospital, which mainly consists of 12 x 1 layout, with some being 3 x 4 + II and 6 x 2 layout, our method achieved the best AUROC among all AF baseline predictions (as shown in Table 2). The overall performance of ECGFounder’s predictions is

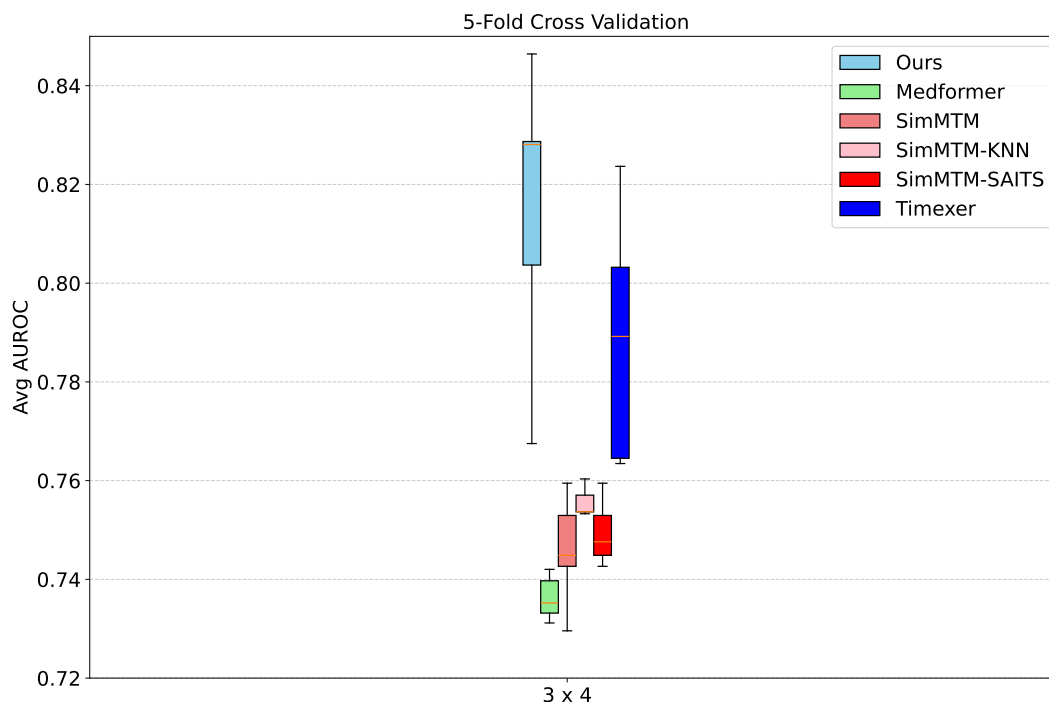


Figure 3: Digitally generated ECG image

good. Although some methods have higher recall rates, their specificity is significantly lower, making them prone to misclassifying negative samples as positive, leading to an increased risk of misdiagnosis. Due to pre-training on tens of millions of ECGs, ECGFounder exhibits strong robustness. When there is a certain degree of data loss, the method fills in the data to a complete 12×1 layout through zero-padding before inputting it into the model. On the external AF cohort of Chaoyang Hospital, the three imputation strategies performed similarly in terms of AUROC scores, with almost no significant differences. This indicates that imputation does not significantly improve the model's accuracy. Medformer performed the best among all baseline methods. This method introduces six data augmentation strategies during the training stage, which act on its internal and external granularity modeling modules, respectively, to enhance the model's robustness to noise and missing data. When dealing with the Chaoyang Hospital cohort with different layouts and poor digitization quality, Medformer achieved an AUROC of 0.605, demonstrating strong adaptability and stability. TimeXer performed well on high-quality digitized signal data, but its performance significantly decreased in the Chaoyang Hospital cohort with poor digitization quality. This method treats missing data as exogenous information and uses it to assist in the modeling and prediction of endogenous information. However, when digitization is poor, not only is the endogenous information itself inaccurate, but the generated missing pattern information also becomes inaccurate. The exogenous information originally used to guide the model becomes a source of interference instead. The introduction of this noise weakens the model's judgment ability, leading to unsatisfactory prediction results on real Chaoyang Hospital image data.

Based on this, we further selected samples arranged in a 12×1 layout for additional evaluation (as shown in Table 3). Our method still achieved the best performance in terms of the AUROC metric, demonstrating strong robustness. ECGFounder achieved the highest recall rate in this 12×1 layout evaluation, exhibiting a strong ability in identifying AF patients and more accurately detecting positive samples. However, its specificity is relatively low, making it prone to misdiagnosing normal individuals as AF patients, posing a certain risk of overdiagnosis. The performance of MedFormer improves with the integrity of lead data, showing significant improvement in the complete 12×1 layout, with a recall rate reaching 0.64. In contrast, the

Table 2: Performance evaluation on an external test set at Chaoyang Hospital

Method	Accuracy	Precision	Recall	Specificity	F1	AUROC
Ours	0.745	0.743	0.750	0.740	0.746	0.778
ECGFounder	0.625	0.605	0.720	0.530	0.658	0.667
SimMTM	0.463	0.332	0.600	0.395	0.427	0.541
SimMTM-KNN	0.485	0.480	0.540	0.430	0.512	0.539
SimMTM-SAITS	0.490	0.491	0.550	0.430	0.519	0.541
Medformer	0.498	0.498	0.640	0.335	0.560	0.605
TimeXer	0.489	0.487	0.460	0.515	0.473	0.485

Table 3: Additional Evaluation of 12 x 1 layout on Chaoyang Hospital test set

Method	Accuracy	Precision	Recall	Specificity	F1	AUROC
Ours	0.833	0.723	0.810	0.845	0.764	0.893
ECGFounder	0.573	0.430	0.860	0.430	0.573	0.703
SimMTM	0.485	0.486	0.525	0.445	0.505	0.450
SimMTM-KNN	–	–	–	–	–	–
SimMTM-SAITS	–	–	–	–	–	–
Medformer	0.450	0.332	0.640	0.355	0.437	0.510
TimeXer	0.473	0.289	0.390	0.510	0.331	0.423

other baseline methods largely fail in scenarios with poor digital quality, struggling to effectively model or make accurate predictions. This further highlights the adaptability and advantages of our method in real complex environments.

Case Study

As shown in Figure 4, we selected ECG image data from Chaoyang Hospital and analyzed it based on its digitized signals. Specifically, it includes the following four typical cases:

(a) In images arranged in a 6×2 layout, the model is capable of accurately identifying key patches. For patches with high attention, a noticeable disappearance of P waves and the appearance of f waves can be observed, indicating that the model can accurately recognize AF characteristics in digitized asynchronous 5s ECG.

(b) Due to the poor quality of the digitalization method used, the digital signal data contains a large amount of noise, which severely interferes with the model mechanism. In this case, the patch that the model focuses on does not exhibit typical AF waveform characteristics, resulting in the misclassification of the AF sample as non-atrial fibrillation (NAF), which is a false negative.

(c) The model correctly classified a NAF sample as NAF. Upon further observation of the patches that the model focused on, we find that it pays attention to patches with atypical waveform changes in some leads, demonstrating its sensitivity to local abnormalities.

(d) In some images, due to poor digitization effects, there is a phenomenon of lead adhesion: the R wave of the lower lead may interfere with the S wave of the upper lead, causing severe jitter in the latter. At the same time, since the model is not trained on digitized data, it may misidentify this abnormal jitter as ST segment deviation. In addition, artifacts may also appear in the P wave region due to digitization distortion, and the model sometimes misidentifies this jitter as an f wave, thereby misdiagnosing NAF samples as AF.

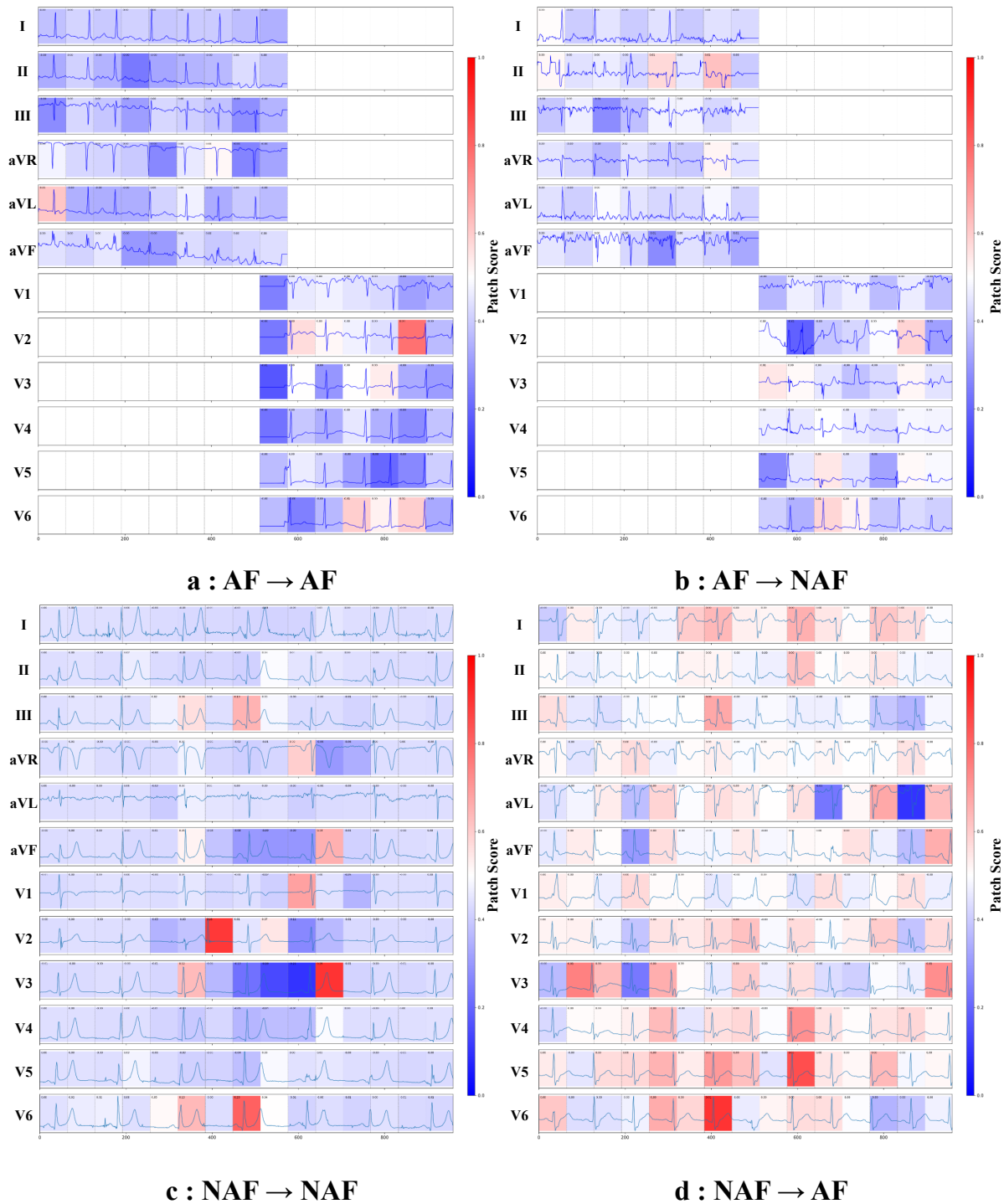


Figure 4: **a**: Accurate prediction of atrial fibrillation; **b**: Misdiagnosis of atrial fibrillation as non-atrial fibrillation; this is a false negative; **c**: Successful identification of non-atrial fibrillation; **d**: Misdiagnosis of non-atrial fibrillation as atrial fibrillation; this is a false positive

DISCUSSION

221

The ECG is an essential tool in cardiological diagnosis, serving as a foundation for detecting and understanding various heart conditions. Despite the continuous advancements in digital ECG equipment, ECG images obtained through photographs, screen captures, or paper still prevail. With the continuous innovation of deep learning in medical research, several studies in the past two years have preliminarily explored methods for processing ECG data with different layouts. However, these methods often simply treat ECGs with different layouts as image classification problems and supplement them with image augmentation techniques. This approach may not only reduce prediction accuracy but also cast doubt on the credibility of model predictions among experts. Compared to image-based predictions, doctors and experts prefer arrhythmia detection based on ECG signals due to their more accurate interpretability. Thanks to advancements in digital methods, ECG image data can be accurately converted into ECG signal data, making it possible to effectively utilize these ECG image resources. Currently, there are numerous excellent research works based on ECG signal predictions, but when digitizing ECGs with different layouts into signals, specific challenges arise - existing methods do not fully consider how to solve the problems brought by signal data with different layouts. How to effectively bridge the gap between the original signal and the digitized signal and address the issue of different layouts will provide more comprehensive insights into ECG images and ECG signals for the future.

222
223
224
225
226
227
228
229
230
231
232
233
234
235
236
237
238

Based on the aforementioned concerns, we propose PatchECG, a novel predictive architecture that addresses arbitrarily layout signal inputs. It combines a masking training strategy and a patch-oriented attention mechanism to achieve intelligent recognition of arbitrarily layouts ECG arrhythmias. We systematically evaluated the proposed method on three types of data, including ECG data with different lead layouts, ECG image signals generated through digitization, and real clinical ECG images from Chaoyang Hospital. In all test scenarios, the model exhibited good predictive performance. Specifically, when training with raw signal data and testing on signal data after image digitization, the model still achieved stable and accurate prediction results⁷. In the external test set from Chaoyang Hospital, which had relatively poor quality, our method achieved an AUC of 0.778 in the AF prediction task, demonstrating strong robustness. Furthermore, when evaluated on additionally filtered synchronous 10-second ECG data, the model's AUC increased to 0.893. The interpretability of the model is of great significance for enhancing clinicians' understanding and trust in AI prediction results.

239
240
241
242
243
244
245
246
247
248
249
250
251

PatchECG provides a comprehensive and adaptable solution for clinical ECG image data and ECG signal data. This solution can accommodate signal data inputs with different layouts, arbitrary lead counts, and lengths. Its design philosophy is rooted in the diagnostic approach of doctors in ECG: when diagnosing specific diseases, doctors pay attention to abnormalities across leads and time segments simultaneously. Our model effectively focuses on key patches, identifying not only obvious abnormal segments in AF samples but also potential atypical waveform areas in some NAF samples. By visually focusing on key patches, the model can provide targeted decision support for clinicians, enhancing the interpretability and practical value of the model.

252
253
254
255
256
257
258
259

Data usage and test setup, we use PTB-XL data as the training data source in this study. There are certain limitations in data usage, which to some extent restrict the model's generalization ability to broader patient populations and more complex pathological types. During the testing phase, we utilize the ECG-image-kit tool to generate ECG images and digitize them to evaluate the model. However, due to limitations in digitization methods, only 3 x 4 layout can be accurately processed, and other layout types of images cannot be effectively digitized. Therefore, in the generated images, we primarily focus on the 3 x 4 layout. In recent years, various digitization methods have emerged, but solutions that truly efficiently and accurately restore high-quality signals remain limited. It is particularly noteworthy that current digitization methods generally lack

260
261
262
263
264
265
266
267
268

effective mechanisms to deal with lead adhesion. When lead adhesion occurs, the signals in the image overlap, which can easily be misjudged by the model as pathological features such as ST segment deviation, leading to deviations in prediction results. Therefore, how to improve the digitization quality of ECG images, especially developing digitization algorithms capable of identifying and correcting lead adhesion issues, is one of the important directions for achieving higher-quality AI-ECG diagnosis research in the future.

In the future, we will further integrate more high-quality and diverse ECG datasets to enhance the generalization ability and clinical applicability of the model. Additionally, given that PatchECG performs better on high-quality digital data, our team has developed the ability to partially reduce the impact of lead adhesion by reconstructing QRS waves. However, this technology is still difficult to fully apply to complex and variable ECG image scenarios. In the future, we will continue to advance the research and development of high-precision, low-noise ECG digitization technology, providing a more accurate signal foundation for downstream AI diagnosis.

CONCLUSION

In this paper, we introduce PatchECG, a method that can be used to detect arrhythmias in ECG with different layouts. Specifically, we have designed an adaptive variable-block missing data representation learning mechanism, combined with a patch-oriented attention mechanism, which automatically focuses on key segments with collaborative dependencies in lead keys. Combined with spatiotemporal embedding, this enables the model to achieve accurate predictions in ECG data with different layouts without introducing additional noise. This method effectively fills the gap in current research regarding the diagnosis of ECGs with different layouts. At the same time, by enhancing the interpretability of key patches, it promotes collaboration between AI and clinicians, facilitating more efficient identification of arrhythmia.

METHODS

292

Related Works

293

Perform Prediction after Interpolation

294

Artificial intelligence has made significant progress in the application of ECG signal arrhythmia detection. Most jobs typically use synchronized 10-s complete ECG signal data, such as using CNNs¹⁶, comparison¹⁷, chen²⁰²⁴congenital, sangha²⁰²²automated, CNN + RNN¹⁷, CNN + Transformer¹⁸ and a hybrid model combining CNN and self-attention mechanism¹⁵, etc. When the input data dimensions are inconsistent, interpolation is usually used to uniformly fill the data to meet the input requirements of the model. Common interpolation strategies include zero padding, traditional machine learning interpolation methods, and deep learning based interpolation methods. SimMTM¹¹, Medformer¹², S4D-ECG¹⁹, CNN + SE¹⁵ and methods such as BiLSTM²⁰ use zero padding strategy to complete missing data before making predictions. These methods can effectively capture the connections between leads and model time-dependent features in synchronizing ECG signal data. Among them, Medformer¹² introduces six data augmentation strategies to make it robust in the face of a certain degree of missing data. In addition, a Random Lead Masking (RLM) training strategy was proposed to ensure stable performance of the model even in the missing of complete leads. By randomly masking a signal segment of about 1.5 seconds, the local loss caused by electrode detachment is simulated to improve the adaptability of the model to small-scale block like loss²¹. Using methods such as KNN and SAITS to interpolate missing data can to some extent complete data completion, allowing for subsequent prediction using existing synchronous 10s ECG signal analysis methods⁹.

295
296
297
298
299
300
301
302
303
304
305
306
307
308
309
310
311
312

However, the above methods all rely on interpolation and modeling strategies. Even with the use of the most advanced interpolation techniques, interpolation errors will still propagate in subsequent modeling, limiting the improvement of model performance. Meanwhile, the uncertainty introduced by interpolation can also reduce the interpretability of prediction results, posing potential challenges for clinical applications.

313
314
315
316
317

Modeling Directly Based on Missing Patterns

318

MissTSM⁹ proposed a new embedding scheme called Time Feature Independent (TFI) embedding, which considers each combination of time steps and features (or channels) as independent labels and encodes them into high-dimensional space, effectively capturing spatiotemporal dependencies without interpolation and achieving direct modeling of missing data. TimeXer introduces external information modeling to enable standard Transformers to coordinate the processing of relationships between internal and external sources¹³. GRU-D proposed a GRU model with attenuation mechanism, which considers missing signals as external signals to enhance the modeling ability of the model on the original time series²². BiTGraph further designed a biased temporal convolutional graph neural network to jointly model temporal dependencies and spatial structural features²³. The above methods can directly model based on missing patterns and effectively capture potential temporal and multivariate dependencies.

319
320
321
322
323
324
325
326
327
328
329

However, these methods face serious challenges when dealing with asynchronous 2.5s and 5s ECG signals caused by different layouts. For example, RNN and GRU-D are prone to gradient vanishing when facing longer sequences; For a large number of continuous Partial Blackout missing in asynchronous ECG, TimeXer and MissSTM will generate a large number of continuous empty tokens, making it difficult for Transformer to effectively predict; In such scenarios, BiTGraph may also have a large number of continuous missing nodes, which affects the coherence and predictive performance of the graph structure. From this, it can be seen that in

330
331
332
333
334
335
336

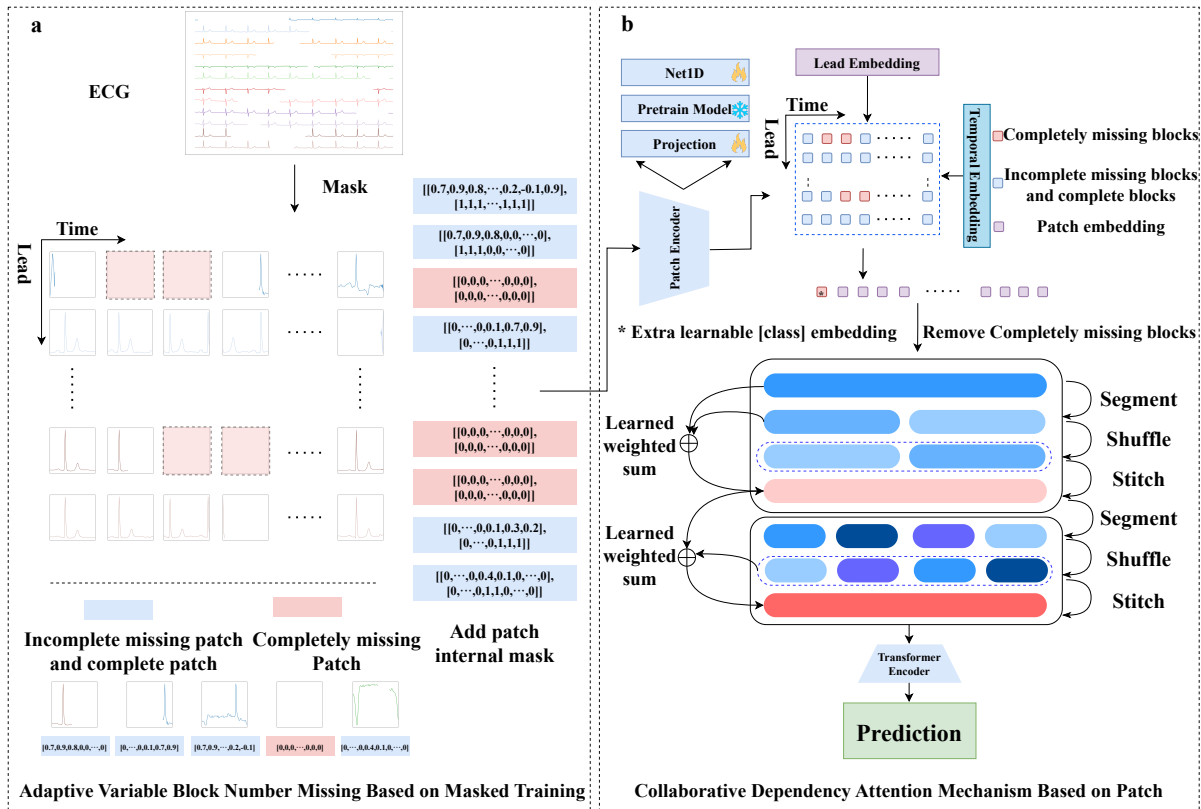


Figure 5: Framework Overview.

scenarios with different layouts of ECG, the above methods are difficult to accurately capture the collaborative dependencies and temporal features between leads, making it difficult to achieve effective modeling of ECG signals. 337 338 339

In summary, although progress has been made in ECG signal data imputation and direct modeling based on missing data, so far there has been no research attempting to solve the asynchronous signal and "Partial Blackout" missing problems caused by different layouts of ECGs. Therefore, this study proposes PatchECG, which designs a novel and universal architecture that adapts to signal data of different layouts, arbitrary lead numbers and lengths without introducing additional noise, and provides interpretability analysis of key patches. This method provides new insights for predicting CVD based on ECGs. 340 341 342 343 344 345 346

Problem Definition 347

Define multi lead ECG data as $X \in \mathbb{R}^{C \times T}$, where C represents the number of ECG leads (electrodes) and T represents the total timestamp. The input is ECG signal data, and the output is multiple possible disease or arrhythmia categories, which belong to the multi label and multi-classification task, that is, each input sample may correspond to multiple category labels at the same time. 348 349 350 351 352

Framework Overview 353

PatchECG is primarily composed of Patch Encoder(PatchEncoder), patch level temporal and lead embedding module, and patch oriented attention module. Figure 5 provides an overview of the PatchECG model proposed in this work. 354 355 356

Adaptive Variable Block Number Missing Based on Masked Training

357

In order to enable the model to effectively learn different layouts of ECG, we propose a masking training strategy to improve the robustness of the model. Before the training starts, mask the ECG data by assigning random starting points, initial positions, and lengths to each lead, and obtain the masked ECG data $\sum_{i=1}^C n_i$.

358

359

360

361

As shown in part a of the Figure 5, first we perform block processing on the data after the mask, and perform equidistant segmentation of the ECG data without coverage, using a window size of P . After segmentation, we obtain N patches, $N = \sum_{i=1}^C n_i$. Among them:

362

363

364

$$n_i = \left\lfloor \frac{c_i}{P} \right\rfloor, C \in \{c_i \mid i = 1, 2 \dots C\} \quad (1)$$

c_i represents the i th lead, n_i represents the number of i th lead blocks, and the last incomplete part is discarded. After cutting, it is divided into three main types of patches: complete patches, partially missing patches, and completely missing patches.

365

366

367

$$m = \left\{ M_{i,j} \in \mathbb{R}^P, i = 1, 2, \dots, C, j = 1, 2, \dots, \left\lfloor \frac{c}{P} \right\rfloor \right\} \quad (2)$$

m represents each block. Add internal markers to each block, generate a marker with the same dimension as the block size based on the missing blocks, with a corresponding value of 1 for existing signals and 0 for missing signals, and perform concatenation, gets \tilde{m}

368

369

370

$$\tilde{m} = \left\{ \tilde{M}_{i,j} \in \mathbb{R}^{2 \times P}, i = 1, 2, \dots, C, j = 1, 2, \dots, \left\lfloor \frac{c}{P} \right\rfloor \right\} \quad (3)$$

Input into PatchEncoder to obtain $\bar{m} \in \mathbb{R}^D$, where D represents the dimension of the embedding layer encoded and output by PatchEncoder for each block. The existing signal based methods include numerous excellent models, which typically take fixed layout and fixed length signals as inputs. We effectively utilize these models and transform them into PatchEncoders to encode the input in patch form. In this way, PatchECG can process ECG signal data with any number of leads, any length, and any layout. We mainly use SE block with attention mechanism as the basic module, combined with Net1d and residual structure to extract high-dimensional features¹⁴.

371

372

373

374

375

376

377

378

Collaborative Dependency Attention Mechanism Based on Patch

379

In our designed model, each block has two inherent features, different leads and different time positions. Unlike simple time series, we need to know the relative position of each block in the ECG. In order to enable PatchECG to better capture the relative position of each patch in the ECG, we initialized a lead embedding list $LE = \{l_0, l_1, \dots, l_C\}$ and a time embedding list $TE = \{t_0, t_1, \dots, t_{\lfloor \frac{c}{P} \rfloor}\}$, Both can be learned during the training process. Add the lead code and time code to \bar{m} to obtain:

380

381

382

383

384

385

$$\bar{m} = \left\{ M_{i,j} + l_i + t_j \mid i = 0, 1, \dots, C, j = 0, 1, \dots, \left\lfloor \frac{C}{P} \right\rfloor \right\} \quad (4)$$

Discard completely missing patches and expand the remaining patches to obtain $\bar{X} \in \mathbb{R}^{(N-N_{miss}) \times D}$, where N_{miss} represents the number of completely missing patches. By optimizing and rearranging \bar{X} to form a new \bar{X}' , potential spatiotemporal dependencies can be better captured. Firstly, segment \bar{X} into multiple segments, then shuffle these segments to optimize the original and shuffled patch sequences through a weighted sum of learnable weights in the

386

387

388

389

390

network. Finally, use the stitch module to connect the shuffled connections and output them to the next layer. Stack them in the neural network to obtain the output \bar{X}'^{24} .

Before inputting into the transformer module, when dividing patches, we mark the blocks and record whether each block is completely missing, all of which are nan. If it is a completely missing block, we choose to discard it directly and only keep the complete and partially missing blocks. Obtain a variable length embedding sequence \bar{X}' , similar to Bert. We add a learnable class embedding to obtain \bar{X}'_{cls} :

$$\bar{X}'_{cls} = [cls : \bar{X}'] \in \mathbb{R}^{(N-N_{miss}+1) \times D} \quad (5)$$

The Transformer Encoder contains many layers (denoted as K layers), and the output of the k-th layer is represented as:

$$\mathbf{H}^{(k)} = \text{TransformerEncoderLayer}(\mathbf{H}^{(k-1)}), \quad k = 1, 2, \dots, K \quad (6)$$

The initial input is:

$$\mathbf{H}^{(0)} = \bar{X}'_{cls} \quad (7)$$

The final result is $\mathbf{H}_{cls}^{(K)} \in \mathbb{R}^{(N-N_{miss}+1) \times E}$, where E represents the output feature dimension. Finally, the prediction using a fully connected layer can be expressed as:

$$\hat{y} = \sigma(\mathbf{H}_{cls}^{(K)}W + b), W \in \mathbb{R}^{E \times R}, b \in \mathbb{R}^R \quad (8)$$

Among them, W and b are trainable parameters, R represents the number of labels for multi label classification, $\sigma(\cdot)$ selects the sigmoid activation function to achieve probability output for multi label and multi-classification, and finally predicts the output:

$$\hat{y} \in \mathbb{R}^R \quad (9)$$

Training

All implementation details match the baseline. We use the exact hyperparameters of the baseline specified in the original paper, or when the code is available. Alternatively, when hyperparameters are not precisely specified in the paper or code, we attempt to maximize performance by searching for the best hyperparameters ourselves. During the training process of PatchECG, the window size P is set to 64, the batch size is set to 64, and the number of training epochs is 30. The optimizer uses Adam, with an initial learning rate of 1×10^{-3} and a weight decay coefficient of 1×10^{-4} . In the PatchEncoder module, the number of basic filters is set to 16, the size of the convolution kernel is 16, and the number of filters in each layer is [16, 32, 32, 40, 40, 64, 64]. Each layer contains two convolution blocks. The hidden feature dimension of the Transformer module is set to 768, with a depth of 3 layers and an 8-head attention mechanism. The S3²⁴ module consists of 3 layers, with an initial number of 4 segments and a segment multiplier of 2. Our code is implemented using PyTorch, and our experiments were conducted on NVIDIA RTX 3090Ti GPU.

Training Data

The data for this study comes from three sources, as shown in Figure 6.

- The dataset used 21388 clinical 12-lead ECGs from 18869 patients using PTB-XL, with each sample lasting 10 seconds. 52% are males and 48% are females, with an age range of 0-95 years old²⁵. We use multi label classification for this data: diagnostic subclasses.

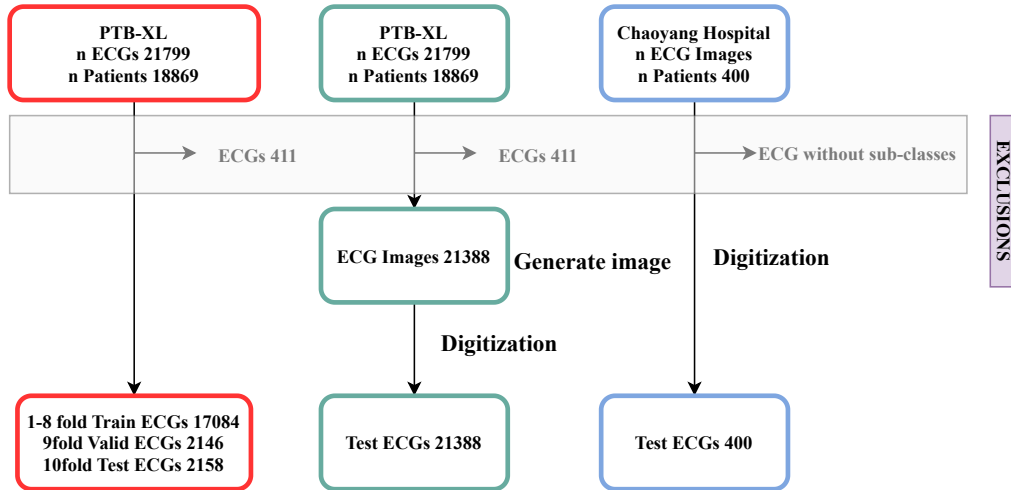


Figure 6: Data used in model development and validation for the ECG arrhythmia detection.

Specifically, the experiment used the official 10 fold split scheme provided by the PTB-XL dataset: in the first round, folds 1-8 were used as the training set, fold 9 as the validation set, and fold 10 as the test set; In the second round, the 7th fold is used as the validation set, the 8th fold is used as the test set, and the remaining folds are used as the training set; Repeat this process for the remaining rounds, rotating the division of the validation and testing sets to complete the evaluation of all folds. Use the Subclass (23 classes) of the multi-class classification task as the label.

- We used the tool provided by ECG-image-kit to generate 21388 ECG images with 3 x 4 layouts of different noise levels on the PTB-XL dataset, and further transformed these images into high-quality ECG signal data that can be used for subsequent analysis using the digital tool⁵, which ranked first in the 2024 CINC competition.
- To evaluate the generalization performance of the model, this study selected a cohort of 400 AF patients admitted to Chaoyang Hospital as an independent external validation set for performance verification. Due to differences in image resolution, size, and layout among the ECG data provided by Chaoyang Hospital, it is difficult to effectively process them using existing automated tools. Therefore, we used Paper ECG⁶ to manually digitize the image data to ensure the accuracy of the signal data.

Evaluation Methods

In our experiment, the task type is the multi-class classification. Specifically, during the model training and evaluation phase, we use the average Area Under the Receiver Operating Characteristic Curve (Avg AUROC) as the main evaluation metric; When conducting external validation on the AF dataset at Chaoyang Hospital, we comprehensively considered multiple indicators such as Accuracy, Precision, Recall, Specification, F1, and AUROC, with a particular focus on recall and specificity performance. In addition, due to significant label imbalance issues in the dataset used, we introduced the Focal Loss loss function²⁶ during the training process: $loss(p) = -\alpha_t(1-p)^\gamma \log p$ To enhance attention to categories with fewer quantities and alleviate the adverse effects of category imbalance.

RESOURCE AVAILABILITY

452

ACKNOWLEDGMENTS

453

This work was supported by the National Natural Science Foundation of China (62102008);
CCF-Zhipu Large Model Innovation Fund (CCF-Zhipu202414).

454

455

DECLARATION OF INTERESTS

456

The authors declare no competing interests.

457

References

1. Mensah, G.A., Roth, G.A., and Fuster, V. (2019). The global burden of cardiovascular diseases and risk factors: 2020 and beyond. American College of Cardiology Foundation Washington, DC.
2. Goldberger, A.L., Amaral, L.A., Glass, L., Hausdorff, J.M., Ivanov, P.C., Mark, R.G., Mietus, J.E., Moody, G.B., Peng, C.K., and Stanley, H.E. (2000). PhysioBank, PhysioToolkit, and PhysioNet: Components of a new research resource for complex physiologic signals. *Circulation* *101*, e215–e220.
3. Sangha, V., Mortazavi, B.J., Haimovich, A.D., Ribeiro, A.H., Brandt, C.A., Jacoby, D.L., Schulz, W.L., Krumholz, H.M., Ribeiro, A.L.P., and Khera, R. (2022). Automated multilabel diagnosis on electrocardiographic images and signals. *Nature communications* *13*, 1583.
4. Gliner, V., Levy, I., Tsutsui, K., Acha, M.R., Schliamser, J., Schuster, A., and Yaniv, Y. (2025). Clinically meaningful interpretability of an ai model for ecg classification. *NPJ Digital Medicine* *8*, 109.
5. Krones, F., Walker, B., Lyons, T., and Mahdi, A. (2024). Combining hough transform and deep learning approaches to reconstruct ecg signals from printouts. *arXiv preprint arXiv:2410.14185*.
6. Fortune, J.D., Coppa, N.E., Haq, K.T., Patel, H., and Tereshchenko, L.G. (2022). Digitizing ecg image: A new method and open-source software code. *Computer methods and programs in biomedicine* *221*, 106890.
7. Sau, A., Zeidaabadi, B., Patlatzoglou, K., Pastika, L., Ribeiro, A.H., Sabino, E., Peters, N.S., Ribeiro, A.L.P., Kramer, D.B., Waks, J.W. et al. (2025). A comparison of artificial intelligence–enhanced electrocardiography approaches for the prediction of time to mortality using electrocardiogram images. *European Heart Journal-Digital Health* *6*, 180–189.
8. Islam, M.R.U., Tadepalli, P., and Fern, A. (2025). Self-attention-based diffusion model for time-series imputation in partial blackout scenarios. In *Proceedings of the AAAI Conference on Artificial Intelligence* vol. 39. pp. 17564–17572.
9. Neog, A., Daw, A., Khorasgani, S.F., and Karpatne, A. (2025). Masking the gaps: An imputation-free approach to time series modeling with missing data. *arXiv preprint arXiv:2502.15785*.
10. Du, W., Côté, D., and Liu, Y. (2023). Saits: Self-attention-based imputation for time series. *Expert Systems with Applications* *219*, 119619.
11. Dong, J., Wu, H., Zhang, H., Zhang, L., Wang, J., and Long, M. (2023). Simmtm: A simple pre-training framework for masked time-series modeling. *Advances in Neural Information Processing Systems* *36*, 29996–30025.
12. Wang, Y., Huang, N., Li, T., Yan, Y., and Zhang, X. (2024). Medformer: A multi-granularity patching transformer for medical time-series classification. *arXiv preprint arXiv:2405.19363*.
13. Wang, Y., Wu, H., Dong, J., Qin, G., Zhang, H., Liu, Y., Qiu, Y., Wang, J., and Long, M. (2024). Timexer: Empowering transformers for time series forecasting with exogenous variables. *arXiv preprint arXiv:2402.19072*.

14. Hong, S., Xu, Y., Khare, A., Priambada, S., Maher, K., Aljiffry, A., Sun, J., and Tumanov, A. (2020). Holmes: Health online model ensemble serving for deep learning models in intensive care units. In Proceedings of the 26th ACM SIGKDD International Conference on Knowledge Discovery & Data Mining. pp. 1614–1624.
15. Li, J., Aguirre, A.D., Junior, V.M., Jin, J., Liu, C., Zhong, L., Sun, C., Clifford, G., Brandon Westover, M., and Hong, S. (2025). An electrocardiogram foundation model built on over 10 million recordings. NEJM AI 2, A0a2401033.
16. Nie, Y., Nguyen, N.H., Sinthong, P., and Kalagnanam, J. (2022). A time series is worth 64 words: Long-term forecasting with transformers. arXiv preprint arXiv:2211.14730.
17. Wang, J., Qiao, X., Liu, C., Wang, X., Liu, Y., Yao, L., and Zhang, H. (2021). Automated ecg classification using a non-local convolutional block attention module. Computer methods and programs in biomedicine 203, 106006.
18. Zhang, S., Lian, C., Xu, B., Su, Y., and Alhudhaif, A. (2024). 12-lead ecg signal classification for detecting ecg arrhythmia via an information bottleneck-based multi-scale network. Information Sciences 662, 120239.
19. Huang, Z., Herbozo Contreras, L.F., Yu, L., Truong, N.D., Nikpour, A., and Kavehei, O. (2024). S4d-ecg: a shallow state-of-the-art model for cardiac abnormality classification. Cardiovascular Engineering and Technology 15, 305–316.
20. Liu, W., Wang, F., Huang, Q., Chang, S., Wang, H., and He, J. (2019). Mfb-cbrnn: A hybrid network for mi detection using 12-lead ecgs. IEEE journal of biomedical and health informatics 24, 503–514.
21. Yao, Q., Wang, R., Fan, X., Liu, J., and Li, Y. (2020). Multi-class arrhythmia detection from 12-lead varied-length ecg using attention-based time-incremental convolutional neural network. Information Fusion 53, 174–182.
22. Che, Z., Purushotham, S., Cho, K., Sontag, D., and Liu, Y. (2018). Recurrent neural networks for multivariate time series with missing values. Scientific reports 8, 6085.
23. Chen, X., Li, X., Liu, B., and Li, Z. (2023). Biased temporal convolution graph network for time series forecasting with missing values. In The Twelfth International Conference on Learning Representations.
24. Grover, S., Jalali, A., and Etemad, A. (2024). Segment, shuffle, and stitch: A simple layer for improving time-series representations. Advances in Neural Information Processing Systems 37, 4878–4905.
25. Wagner, P., Strodthoff, N., Bousseljot, R.D., Kreiseler, D., Lunze, F.I., Samek, W., and Schaeffter, T. (2020). Ptb-xl, a large publicly available electrocardiography dataset. Scientific data 7, 1–15.
26. Lin, T.Y., Goyal, P., Girshick, R., He, K., and Dollár, P. (2017). Focal loss for dense object detection. In Proceedings of the IEEE international conference on computer vision. pp. 2980–2988.